26 KSME Journal, Vol. 7, No. 1, pp. 26~34, 1993

Joint Coordinate Method for Analysis and Design of Multibody Systems : Part 2. System Topology

Gwanghun Gim* and Parviz E. Nikravesh**

(Received July 13, 1992)

In Part 1 of this paper, the method of joint coordinate formulation for multibody dynamics was reviewed. The application of this method to forward and inverse dynamics, static equilibrium, and design sensitivity analyses was studied. In Part 2 of the paper, systematic procedures for constructing the necessary matrices for the joint coordinate formulation are discussed in detail. These matrices are ; the primary and the secondary path matrices describing the topology of the system, the velocity transformation matrix, and the generalized inertia matrix. The procedures for constructing these matrices and other necessary elements for the joint coordinate formulation can easily be implemented in a computer program for analysis and design process.

Key Words: Topology, Path Matrix, Velocity Transformation Matrix, Generalized Inertia Matrix

1. Introduction

In Part 1 of this paper (Gim and Nikravesh, 1993), a linear velocity transformation matrix is described as the relationship between the joint and the absolute velocities of a multibody system. The derivation of the equations of motion for forward and inverse dynamics is shown. Expressions for evaluating reaction and actuator forces at a kinematic joint are derived using joint coordinate method. An application of the joint coordinate method to static equilibrium and design sensitivity analyses are also studied.

In Part 2, a method for constructing the velocity transformation matrix from block matrices representing the system kinematics is shown. A systematic generation of the velocity transformation matrix employs a path matrix representing the system topology. Using a graphical representation, the path matrix is constructed to describe the characteristics of system topology. Detailed description of the generalized inertia matrix and a process for its systematic construction is also presented.

* R & D Center, Hankook Tire Mfg. Co., Ltd. Taejon, 305-343, Republic of Korea

** Department of Aerospace and Mechanical Engineering, University of Arizona, Tucson, AZ 85721, U.S.A.

2. Path Matrix

The topology and kinematical propeties of a large-scale multibody system can be efficiently represented by a graph. In the graphical representation of a multibody system, each body is considered as a node (or vertex) while each kinematic joint is defined as an edge. Each open-loop is represented by a branch, but each closed-loop may be represented by one or two branches depending on the location of a cut joint in the closed-loop. Each tree starts from a root toward a leaf corresponding to the topological path which starts from a base body toward a leaf body. The graphical representation employs a path matrix

which contains the characteristics of the system topology. Row i and column j of the path matrix correspond to node i and edge j respectively. If the path matrix and its elements are denoted by $\boldsymbol{I}_g$ and g_{ij} respectively, then g_{ij} is defined as

$$g_{ij}=\begin{cases} 1; \text{ if edge } j \text{ is directed away from node } i, \\ -1; \text{ if edge } j \text{ is directed toward node } i, \\ 0; \text{ otherwise.} \end{cases}$$

For convenience, the ground is considered as node 0 which is not included in path matrix $\boldsymbol{I}_g$. A floating base body is assumed to be connected to node 0 through an edge. This edge represents an integration which determines the coordinates of the floating base body. Furthermore, the edges should be numbered in sequential order according to the order of the path though kinematic joints do not.

In order to show the construction process of a path matrix, the Stanford manipulator and its graphical representation are shown in Fig. 2.1. This system contains six moving bodies and six kinematic joints. Bodies 1 through 6 are connected to the ground by five revolute joints, R_1, R_2, R_4, R_5, and R_6, and a prismatic joint T_3. Based on the graph, a path matrix $\boldsymbol{I}_g$ is obtained as

$$\boldsymbol{I}_g=\begin{array}{c|cccccc|} & [1] & [2] & [3] & [4] & [5] & [6] & \\ (1) & -1 & 1 & 0 & 0 & 0 & 0 & \\ (2) & 0 & -1 & 1 & 0 & 0 & 0 & \\ (3) & 0 & 0 & -1 & 1 & 0 & 0 & \\ (4) & 0 & 0 & 0 & -1 & 1 & 0 & \\ (5) & 0 & 0 & 0 & 0 & -1 & 1 & \\ (6) & 0 & 0 & 0 & 0 & 0 & -1 & (6\times 6) \end{array} \tag{2.1}$$

where row (i) and column $[j]$, for $i=1,6$, correspond to node i and edge j respectively.

As another example, a double-wishbone suspension system and its graphical representation are given in Fig. 2.2. The main chassis is defined as a floating base body, and the knuckle is connected to the main chassis via two revolute joints, R_2 and R_5, and two spherical joints, S_3 and S_6, which comprises a closed-loop. A wheel is then connected to the knuckle by revolute joint R_4. If

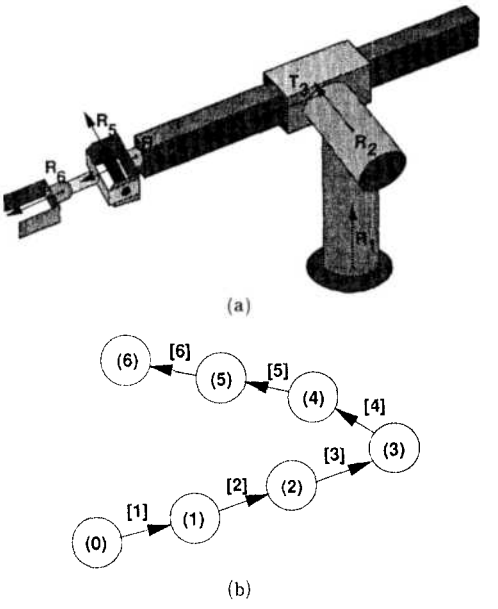

Fig. 2.1 (a) Stanford manipulator and (b) its graphical representation

the closed-loop is cut at S_6, then its reduced open-loop system is represented by two branches as shown in Fig. 2.2(b). The path matrix $\boldsymbol{I}_g$ is thus determined as

$$\boldsymbol{I}_g=\begin{array}{c|ccccc|} & [1] & [2] & [3] & [4] & [5] & \\ (1) & -1 & 1 & 0 & 0 & 1 & \\ (2) & 0 & -1 & 1 & 0 & 0 & \\ (3) & 0 & 0 & -1 & 1 & 0 & \\ (4) & 0 & 0 & 0 & -1 & 0 & \\ (5) & 0 & 0 & 0 & 0 & -1 & (5\times 5) \end{array} \tag{2.2}$$

Note that the first column of the path matrix always contains only one -1 and the rest are 0's. Also a kinematic joint connected to the ground is represented by a column that has only one -1 and the rest are 0's. If there exists more than one floating base body, each column corresponding to each floating base body has only one -1 and 0's. Otherwise, each column contains one 1, one -1, and 0's.

In order to show how a path matrix can be used to find a closed-loop in case the cut joint is not selected, one possible graphical representation of the above example is given in Fig. 2.2(c). Its path

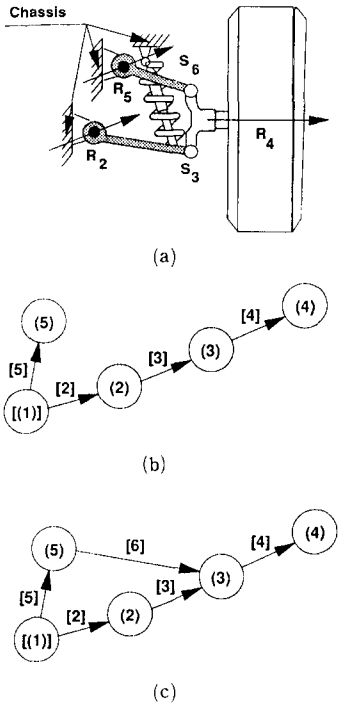

Fig. 2.2 (a) A double-wishbone suspension system, (b) the graphical representation of its reduced open-loop system, and (c) the graphical representation of its closedloop system

matrix I_o becomes

$$I_o = \begin{array}{c|cccccc|} & [1] & [2] & [3] & [4] & [5] & [6] \\ (1) & -1 & 1 & 0 & 0 & 1 & 0 \\ (2) & 0 & -1 & 1 & 0 & 0 & 0 \\ (3) & 0 & 0 & -1 & 1 & 0 & -1 \\ (4) & 0 & 0 & 0 & -1 & 0 & 0 \\ (5) & 0 & 0 & 0 & 0 & -1 & 1 \end{array} \quad (5\times 6) \tag{2.3}$$

From Eq. (2.3) it is observed that two - 1's at row (3) indicate a closed-loop because node 3 has two up-trees which has only one root. If joint S_6 is chosen as a cut joint, column [6] is eliminated from Eq. (2.3) and then Eq. (2.3) becomes identical to Eq. (2.2).

In this example we have four candidates for a cut joint such as joints R_2, S_3, R_5, and S_6. To be a cut joint, joint R_2 or R_5 requires five kinematic constraints, while joint S_3 or S_6 requires only three kinematic constraints. Furthermore, joint R_2 or R_5 provides only one joint coordinate, while joint S_3 or S_6 furnishes three joint coordinates. Therefore, joint S_3 or S_6 should be selected for better effectiveness. The choice of a cut joint is also dependent on the inertia properties of its adjacent bodies. A computer algorithm has been successfully implemented to produce automatically the path matrix of the reduced open-loop system of a large-scale multibody system containing closed-loops.

At the next stage, matrix I_o is modified in order to get all the necessary information on the connectivity and path flow of the system. The algorithm for constructing a secondary path matrix I_o^* is:

(a) Initially set a counter $j=2$ for the column of matrix I_o.

(b) In column j, find row m having 1 and row n having -1.

(c) If $g_{mk}<0$ for $k=1, j-1$, then perform $g_{nk}=g_{nk}+g_{mk}-1$.

(d) If j is equal to the total number of columns, replace all the 1's with 0's and then stop.

(e) Otherwise, set $j=j+1$ and go to (b).

Based on the above algorithm, for the Stanford manipulator, the path matrix of Eq. (2.1) is changed to

$$I_o^* = \begin{array}{c|cccccc|} & [1] & [2] & [3] & [4] & [5] & [6] \\ (1) & -1 & 0 & 0 & 0 & 0 & 0 \\ (2) & -2 & -1 & 0 & 0 & 0 & 0 \\ (3) & -3 & -2 & -1 & 0 & 0 & 0 \\ (4) & -4 & -3 & -2 & -1 & 0 & 0 \\ (5) & -5 & -4 & -3 & -2 & -1 & 0 \\ (6) & -6 & -5 & -4 & -3 & -2 & -1 \end{array} \quad (6\times 6) \tag{2.4}$$

Similarly, for the suspension system, the path matrix of Eq. (2.2) becomes

$$I_o^* = \begin{array}{c|ccccc|} & [1] & [2] & [3] & [4] & [5] \\ (1) & -1 & 0 & 0 & 0 & 0 \\ (2) & -2 & -1 & 0 & 0 & 0 \\ (3) & -3 & -2 & -1 & 0 & 0 \\ (4) & -4 & -3 & -2 & -1 & 0 \\ (5) & -2 & 0 & 0 & 0 & -1 \end{array} \quad (5\times 5) \tag{2.5}$$

In matrix I_o^*, negative integer entries provide all necessary information on the connectivity of a

multibody system, and also the numeric order of the negative integer entries indicates the path flow of the system. In column j, rows which have negative integer entries indicate the nodes connecting to the root by edge j. A row which has -1 indicates the first node connected to edge j, while a row which contains the smallest negative integer indicates the last node. The same negative integer entries in a column indicates more than one branch. Since the path matrix contains all necessary information on the system topology, it can be used to construct the velocity transformation matrix $\boldsymbol{B}$.

3.Velocity Transformation Matrix

Velocity transformation matrix $\boldsymbol{B}$ depends on the kinematics and the topology of a multibody system. If block matrix $\boldsymbol{B}_{ij}$ is defined to represent the local properties of a kinematic joint, then matrix $\boldsymbol{B}$ can be obtained by assembling block matrices $\boldsymbol{B}_{ij}$'s based on the system topology. Block matrices are determined for a floating base body and various kinematic joints as shown in Table 2.1 (Kim and Vanderploeg, 1986), where subscript i stands for body i (or node i) and subscript j stands for floating base body j or kinematic joint j (or edge j). It is noted that the block matrix $\boldsymbol{B}_{ij}$ for a composite joint is determined as a combination of those of a revoloute and a prismatic joint. For a floating base body, a vector of absolute coordinates is defined as the joint coordinates, while for kinematic joints relative joint coordinates are used. Vector $\boldsymbol{d}_{ij}$ is defined as a vector toward the center of mass of body i from the center of mass of the floating base

Table 2.1 Block matrix $\boldsymbol{B}_{ij}$

Type of Joint j	ID Symbols	Joint Velocities	Joint Axes	Matrix Size	$\boldsymbol{B}_{ij}$
Floating Base Body	$\boldsymbol{F}_{ij}$	$\begin{bmatrix} \dot{\boldsymbol{r}}_j \\ \boldsymbol{\omega}_j \end{bmatrix}$	Global xyz Coordinates	6×6	$\begin{bmatrix} \boldsymbol{I} & -\tilde{\boldsymbol{d}}_{ij} \\ \boldsymbol{0} & \boldsymbol{I} \end{bmatrix}$
Spherical Joint	$\boldsymbol{S}_{ij}$	$\boldsymbol{\omega}_j^{(r)}$	Global xyz Coordinates	6×3	$\begin{bmatrix} -\tilde{\boldsymbol{d}}_{ij} \\ \boldsymbol{I} \end{bmatrix}$
Revolute Joint	$\boldsymbol{R}_{ij}$	$\dot{\theta}_j$	$\boldsymbol{u}_j$	6×1	$\begin{bmatrix} -\tilde{\boldsymbol{d}}_{ij}\boldsymbol{u}_j \\ \boldsymbol{u}_j \end{bmatrix}$
Prismatic Joint	$\boldsymbol{P}_{ij}$	$\dot{\theta}_j$	$\boldsymbol{u}_j$	6×1	$\begin{bmatrix} \boldsymbol{u}_j \\ \boldsymbol{0} \end{bmatrix}$
Rev.-Rev. Joint	$\boldsymbol{C}_{ij}^{R-R}$	$\begin{bmatrix} \dot{\theta}_j^{(1)} \\ \dot{\theta}_j^{(2)} \end{bmatrix}$	$[\boldsymbol{u}_j^{(1)}, \boldsymbol{u}_j^{(2)}]^1$	6×2	$\begin{bmatrix} -\tilde{\boldsymbol{d}}_{ij}^{(1)}\boldsymbol{u}_j^{(1)} & -\tilde{\boldsymbol{d}}_{ij}^{(2)}\boldsymbol{u}_j^{(2)} \\ \boldsymbol{u}_j^{(1)} & \boldsymbol{u}_j^{(2)} \end{bmatrix}$
Pri.-Rev. Joint	$\boldsymbol{C}_{ij}^{P-R}$	$\begin{bmatrix} \dot{\theta}_j^{(1)} \\ \dot{\theta}_j^{(2)} \end{bmatrix}$	$[\boldsymbol{u}_j^{(1)}, \boldsymbol{u}_j^{(2)}]^2$	6×2	$\begin{bmatrix} \boldsymbol{u}_j^{(1)} & -\tilde{\boldsymbol{d}}_{ij}^{(2)}\boldsymbol{u}_j^{(2)} \\ \boldsymbol{0} & \boldsymbol{u}_j^{(2)} \end{bmatrix}$
Rev.-Pri. Joint	$\boldsymbol{C}_{ij}^{R-P}$	$\begin{bmatrix} \dot{\theta}_j^{(1)} \\ \dot{\theta}_j^{(2)} \end{bmatrix}$	$[\boldsymbol{u}_j^{(1)}, \boldsymbol{u}_j^{(2)}]$	6×2	$\begin{bmatrix} -\tilde{\boldsymbol{d}}_{ij}^{(1)}\boldsymbol{u}_j^{(1)} & \boldsymbol{u}_j^{(2)} \\ \boldsymbol{u}_j^{(1)} & \boldsymbol{0} \end{bmatrix}$

Note:

1. If a revolute-revolute joint has $\boldsymbol{u}_j^{(1)T}\boldsymbol{u}_j^{(2)}=0$ and $\boldsymbol{d}_{ij}^{(1)}=\boldsymbol{d}_{ij}^{(2)}$, then it becomes a universal joint.
2. If a prismatic-revolute joint has $\boldsymbol{u}_j^{(1)}=\boldsymbol{u}_j^{(2)}$, then it becomes a cylindrical joint.

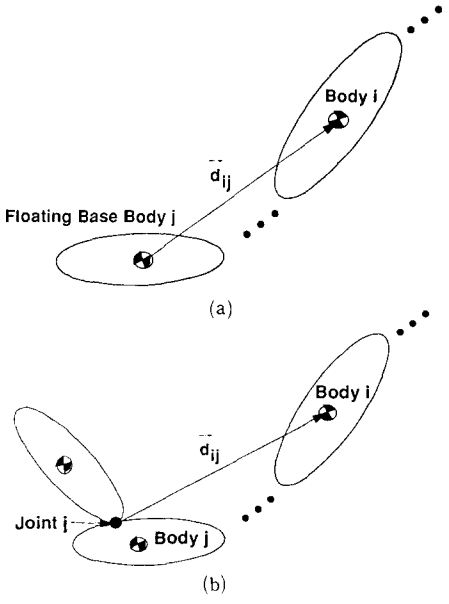

Fig. 2.3 A schematic representation of vector $\boldsymbol{d}_{ij}$ for ; (a) a floating base body and (b) a kinematic joint

body j, or from the attachment point of joint j (see Fig. 2.3). If body i is the same as the floating base body j, then $\boldsymbol{d}_{ij}=\mathbf{0}$.

For the purpose of illustrating the construction of various block matrices, previous two examples are considered here. For the Stanford manipulator (refer to Fig. 2.1), θ_j, for $j=1,6$, is defined as a vector of joint coordinates shown in Fig. 2.4. The joint coordinates, θ_1, θ_2, θ_4, θ_5, and θ_6, are relative rotational coordinates about revolute joints, R_1, R_2, R_4, R_5, and R_6, where θ_3 is a relative translational coordinate along a prismatic joint T_3. The absolute velocities of the bodies in the system can thus be determined in terms of joint velocities.

For the angular velocities, we have

$$\begin{aligned}
\boldsymbol{\omega}_1&=\boldsymbol{u}_1\dot{\theta}_1,\\
\boldsymbol{\omega}_2&=\boldsymbol{\omega}_1+\boldsymbol{u}_2\dot{\theta}_2,\\
\boldsymbol{\omega}_3&=\boldsymbol{\omega}_2,\\
\boldsymbol{\omega}_4&=\boldsymbol{\omega}_3+\boldsymbol{u}_4\dot{\theta}_4,\\
\boldsymbol{\omega}_5&=\boldsymbol{\omega}_4+\boldsymbol{u}_5\dot{\theta}_5,\\
\boldsymbol{\omega}_6&=\boldsymbol{\omega}_5+\boldsymbol{u}_6\dot{\theta}_6.
\end{aligned}\tag{2.6}$$

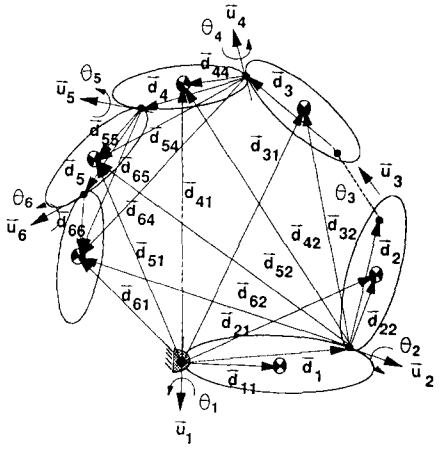

Fig. 2.4 A schematic representation of Stanford manipulator for the joint coordinates

To obtain expressions for the absolute translational velocities as a function of the joint velocities, as an example, the derivation for body 6 is shown in detail. The translational coordinates of body 6 can be expressed as

$$\boldsymbol{r}_6=\boldsymbol{d}_1+\boldsymbol{d}_2+\boldsymbol{u}_3\theta_3+\boldsymbol{d}_3+\boldsymbol{d}_4+\boldsymbol{d}_5+\boldsymbol{d}_6.$$

Its time derivative gives an expression for the translational velocities as

$$\begin{aligned}
\dot{\boldsymbol{r}}_6&=\dot{\boldsymbol{d}}_1+\dot{\boldsymbol{d}}_2+\dot{\boldsymbol{u}}_3\theta_3+\boldsymbol{u}_3\dot{\theta}_3+\dot{\boldsymbol{d}}_3+\dot{\boldsymbol{d}}_4+\dot{\boldsymbol{d}}_5+\dot{\boldsymbol{d}}_6,\\
&=-\tilde{\boldsymbol{d}}_1\boldsymbol{\omega}_1-\tilde{\boldsymbol{d}}_2\boldsymbol{\omega}_2-\tilde{\boldsymbol{u}}_3\boldsymbol{\omega}_2\theta_3+\boldsymbol{u}_3\dot{\theta}_3\\
&\quad-\tilde{\boldsymbol{d}}_3\boldsymbol{\omega}_3-\tilde{\boldsymbol{d}}_4\boldsymbol{\omega}_4-\tilde{\boldsymbol{d}}_5\boldsymbol{\omega}_5-\tilde{\boldsymbol{d}}_6\boldsymbol{\omega}_6,
\end{aligned}$$

where $\tilde{\boldsymbol{d}}$ is a skew-symmetric matrix associated with the components of vector $\boldsymbol{d}=[d_1,\ d_2,\ d_3]^T$, which is defined for vector product operation as

$$\tilde{\boldsymbol{d}}\equiv\begin{bmatrix}0&-d_3&d_2\\d_3&0&-d_1\\-d_2&d_1&0\end{bmatrix}(3\times3).$$

Now substituting Eq. (2.6) in the expression for $\dot{\boldsymbol{r}}_6$ yields

$$\begin{aligned}
\dot{\boldsymbol{r}}_6=&-(\tilde{\boldsymbol{d}}_1+\tilde{\boldsymbol{d}}_2+\tilde{\boldsymbol{u}}_3\theta_3+\tilde{\boldsymbol{d}}_3+\tilde{\boldsymbol{d}}_4+\tilde{\boldsymbol{d}}_5+\tilde{\boldsymbol{d}}_6)\boldsymbol{u}_1\dot{\theta}_1\\
&-(\tilde{\boldsymbol{d}}_2+\tilde{\boldsymbol{u}}_3\theta_3+\tilde{\boldsymbol{d}}_3+\tilde{\boldsymbol{d}}_4+\tilde{\boldsymbol{d}}_5+\tilde{\boldsymbol{d}}_6)\boldsymbol{u}_2\dot{\theta}_2\\
&+\boldsymbol{u}_3\dot{\theta}_3-(\tilde{\boldsymbol{d}}_4+\tilde{\boldsymbol{d}}_5+\tilde{\boldsymbol{d}}_6)\boldsymbol{u}_4\dot{\theta}_4\\
&-(\tilde{\boldsymbol{d}}_5+\tilde{\boldsymbol{d}}_6)\boldsymbol{u}_5\dot{\theta}_5-\tilde{\boldsymbol{d}}_6\boldsymbol{u}_6\dot{\theta}_6,
\end{aligned}$$

or

$$\begin{aligned}
\dot{\boldsymbol{r}}_6=&-\tilde{\boldsymbol{d}}_{61}\boldsymbol{u}_1\dot{\theta}_1-\tilde{\boldsymbol{d}}_{62}\boldsymbol{u}_2\dot{\theta}_2+\boldsymbol{u}_3\dot{\theta}_3-\tilde{\boldsymbol{d}}_{64}\boldsymbol{u}_4\dot{\theta}_4\\
&-\tilde{\boldsymbol{d}}_{65}\boldsymbol{u}_5\dot{\theta}_5-\tilde{\boldsymbol{d}}_{66}\boldsymbol{u}_6\dot{\theta}_6,
\end{aligned}$$

where $\boldsymbol{d}_6=\boldsymbol{d}_{66}$ and vectors $\boldsymbol{d}_{ij}$'s are shown in Fig. 2.4. This process can be repeated for all the bodies to obtain a complete set of absolute translational velocities as

$$\begin{aligned}
\dot{\boldsymbol{r}}_1&=-\tilde{\boldsymbol{d}}_{11}\boldsymbol{u}_1\dot{\theta}_1,\\
\dot{\boldsymbol{r}}_2&=-\tilde{\boldsymbol{d}}_{21}\boldsymbol{u}_1\dot{\theta}_1-\tilde{\boldsymbol{d}}_{22}\boldsymbol{u}_2\dot{\theta}_2,\\
\dot{\boldsymbol{r}}_3&=-\tilde{\boldsymbol{d}}_{31}\boldsymbol{u}_1\dot{\theta}_1-\tilde{\boldsymbol{d}}_{32}\boldsymbol{u}_2\dot{\theta}_2+\boldsymbol{u}_3\dot{\theta}_3,\\
\dot{\boldsymbol{r}}_4&=-\tilde{\boldsymbol{d}}_{41}\boldsymbol{u}_1\dot{\theta}_1-\tilde{\boldsymbol{d}}_{42}\boldsymbol{u}_2\dot{\theta}_2+\boldsymbol{u}_3\dot{\theta}_3-\tilde{\boldsymbol{d}}_{44}\boldsymbol{u}_4\dot{\theta}_4,\\
\dot{\boldsymbol{r}}_5&=-\tilde{\boldsymbol{d}}_{51}\boldsymbol{u}_1\dot{\theta}_1-\tilde{\boldsymbol{d}}_{52}\boldsymbol{u}_2\dot{\theta}_2+\boldsymbol{u}_3\dot{\theta}_3-\tilde{\boldsymbol{d}}_{54}\boldsymbol{u}_4\dot{\theta}_4\\
&\quad-\tilde{\boldsymbol{d}}_{55}\boldsymbol{u}_5\dot{\theta}_5,\\
\dot{\boldsymbol{r}}_6&=-\tilde{\boldsymbol{d}}_{61}\boldsymbol{u}_1\dot{\theta}_1-\tilde{\boldsymbol{d}}_{62}\boldsymbol{u}_2\dot{\theta}_2+\boldsymbol{u}_3\dot{\theta}_3-\tilde{\boldsymbol{d}}_{64}\boldsymbol{u}_4\dot{\theta}\\
&\quad-\tilde{\boldsymbol{d}}_{65}\boldsymbol{u}_5\dot{\theta}_5-\tilde{\boldsymbol{d}}_{66}\boldsymbol{u}_6\dot{\theta}_6.
\end{aligned}\tag{2.7}$$

From Eqs. (2.6) and (2.7), the vector of absolute velocities can be written as a function of the vector of joint velocities ; i.e.,

$$\begin{bmatrix}\dot{\boldsymbol{r}}_1\\ \boldsymbol{\omega}_1\\ \dot{\boldsymbol{r}}_2\\ \boldsymbol{\omega}_2\\ \dot{\boldsymbol{r}}_3\\ \boldsymbol{\omega}_3\\ \dot{\boldsymbol{r}}_4\\ \boldsymbol{\omega}_4\\ \dot{\boldsymbol{r}}_5\\ \boldsymbol{\omega}_5\\ \dot{\boldsymbol{r}}_6\\ \boldsymbol{\omega}_6\end{bmatrix}=\begin{bmatrix}
-\tilde{\boldsymbol{d}}_{11}\boldsymbol{u}_1 & \boldsymbol{0} & \boldsymbol{0} & \boldsymbol{0} & \boldsymbol{0} & \boldsymbol{0}\\
\boldsymbol{u}_1 & \boldsymbol{0} & \boldsymbol{0} & \boldsymbol{0} & \boldsymbol{0} & \boldsymbol{0}\\
-\tilde{\boldsymbol{d}}_{21}\boldsymbol{u}_1 & -\tilde{\boldsymbol{d}}_{22}\boldsymbol{u}_2 & \boldsymbol{0} & \boldsymbol{0} & \boldsymbol{0} & \boldsymbol{0}\\
\boldsymbol{u}_1 & \boldsymbol{u}_2 & \boldsymbol{0} & \boldsymbol{0} & \boldsymbol{0} & \boldsymbol{0}\\
-\tilde{\boldsymbol{d}}_{31}\boldsymbol{u}_1 & -\tilde{\boldsymbol{d}}_{32}\boldsymbol{u}_2 & \boldsymbol{u}_3 & \boldsymbol{0} & \boldsymbol{0} & \boldsymbol{0}\\
\boldsymbol{u}_1 & \boldsymbol{u}_2 & \boldsymbol{0} & \boldsymbol{0} & \boldsymbol{0} & \boldsymbol{0}\\
-\tilde{\boldsymbol{d}}_{41}\boldsymbol{u}_1 & -\tilde{\boldsymbol{d}}_{42}\boldsymbol{u}_2 & \boldsymbol{u}_3 & -\tilde{\boldsymbol{d}}_{44}\boldsymbol{u}_4 & \boldsymbol{0} & \boldsymbol{0}\\
\boldsymbol{u}_1 & \boldsymbol{u}_2 & \boldsymbol{0} & \boldsymbol{u}_4 & \boldsymbol{0} & \boldsymbol{0}\\
-\tilde{\boldsymbol{d}}_{51}\boldsymbol{u}_1 & -\tilde{\boldsymbol{d}}_{52}\boldsymbol{u}_2 & \boldsymbol{u}_3 & -\tilde{\boldsymbol{d}}_{54}\boldsymbol{u}_4 & -\tilde{\boldsymbol{d}}_{55}\boldsymbol{u}_5 & \boldsymbol{0}\\
\boldsymbol{u}_1 & \boldsymbol{u}_2 & \boldsymbol{0} & \boldsymbol{u}_4 & \boldsymbol{u}_5 & \boldsymbol{0}\\
-\tilde{\boldsymbol{d}}_{61}\boldsymbol{u}_1 & -\tilde{\boldsymbol{d}}_{62}\boldsymbol{u}_2 & \boldsymbol{u}_3 & -\tilde{\boldsymbol{d}}_{64}\boldsymbol{u}_4 & -\tilde{\boldsymbol{d}}_{65}\boldsymbol{u}_5 & -\tilde{\boldsymbol{d}}_{66}\boldsymbol{u}_6\\
\boldsymbol{u}_1 & \boldsymbol{u}_2 & \boldsymbol{0} & \boldsymbol{u}_4 & \boldsymbol{u}_5 & \boldsymbol{u}_6
\end{bmatrix}\begin{bmatrix}\dot{\theta}_1\\ \dot{\theta}_2\\ \dot{\theta}_3\\ \dot{\theta}_4\\ \dot{\theta}_5\\ \dot{\theta}_6\end{bmatrix}$$

Comparing this equation with $\boldsymbol{v}=\boldsymbol{B}\dot{\boldsymbol{\theta}}$ yields

$$\boldsymbol{B}=\begin{bmatrix}
-\tilde{\boldsymbol{d}}_{11}\boldsymbol{u}_1 & \boldsymbol{0} & \boldsymbol{0} & \boldsymbol{0} & \boldsymbol{0} & \boldsymbol{0}\\
\boldsymbol{u}_1 & \boldsymbol{0} & \boldsymbol{0} & \boldsymbol{0} & \boldsymbol{0} & \boldsymbol{0}\\
-\tilde{\boldsymbol{d}}_{21}\boldsymbol{u}_1 & -\tilde{\boldsymbol{d}}_{22}\boldsymbol{u}_2 & \boldsymbol{0} & \boldsymbol{0} & \boldsymbol{0} & \boldsymbol{0}\\
\boldsymbol{u}_1 & \boldsymbol{u}_2 & \boldsymbol{0} & \boldsymbol{0} & \boldsymbol{0} & \boldsymbol{0}\\
-\tilde{\boldsymbol{d}}_{31}\boldsymbol{u}_1 & -\tilde{\boldsymbol{d}}_{32}\boldsymbol{u}_2 & \boldsymbol{u}_3 & \boldsymbol{0} & \boldsymbol{0} & \boldsymbol{0}\\
\boldsymbol{u}_1 & \boldsymbol{u}_2 & \boldsymbol{0} & \boldsymbol{0} & \boldsymbol{0} & \boldsymbol{0}\\
-\tilde{\boldsymbol{d}}_{41}\boldsymbol{u}_1 & -\tilde{\boldsymbol{d}}_{42}\boldsymbol{u}_2 & \boldsymbol{u}_3 & -\tilde{\boldsymbol{d}}_{44}\boldsymbol{u}_4 & \boldsymbol{0} & \boldsymbol{0}\\
\boldsymbol{u}_1 & \boldsymbol{u}_2 & \boldsymbol{0} & \boldsymbol{u}_4 & \boldsymbol{0} & \boldsymbol{0}\\
-\tilde{\boldsymbol{d}}_{51}\boldsymbol{u}_1 & -\tilde{\boldsymbol{d}}_{52}\boldsymbol{u}_2 & \boldsymbol{u}_3 & -\tilde{\boldsymbol{d}}_{54}\boldsymbol{u}_4 & -\tilde{\boldsymbol{d}}_{55}\boldsymbol{u}_5 & \boldsymbol{0}\\
\boldsymbol{u}_1 & \boldsymbol{u}_2 & \boldsymbol{0} & \boldsymbol{u}_4 & \boldsymbol{u}_5 & \boldsymbol{0}\\
-\tilde{\boldsymbol{d}}_{61}\boldsymbol{u}_1 & -\tilde{\boldsymbol{d}}_{62}\boldsymbol{u}_2 & \boldsymbol{u}_3 & -\tilde{\boldsymbol{d}}_{64}\boldsymbol{u}_4 & -\tilde{\boldsymbol{d}}_{65}\boldsymbol{u}_5 & -\tilde{\boldsymbol{d}}_{66}\boldsymbol{u}_6\\
\boldsymbol{u}_1 & \boldsymbol{u}_2 & \boldsymbol{0} & \boldsymbol{u}_4 & \boldsymbol{u}_5 & \boldsymbol{u}_6
\end{bmatrix}\quad(36\times 6)\tag{2.8}$$

As a second example, the double-wishbone suspension system of Fig. 2.2 is shown schematically in Fig. 2.5. For the main chassis as a floating base body, vectors of absolute translational and angular velocities, $\dot{\boldsymbol{r}}_1$ and $\boldsymbol{\omega}_1$, are defined as joint velocities, while at the revolute joints, R_2, R_4, and R_5, relative rotational velocities, $\dot{\theta}_2$, $\dot{\theta}_4$, and $\dot{\theta}_5$, are defined as joint velocities. At the spherical joint S_3, a vector of relative angular velocities $\boldsymbol{\omega}_3^{(r)}$ between bodies 2 and 3 that share the spherical joint is defined as the joint velocities. The absolute angular velocities of bodies in the system can also be obtained as

$$\begin{aligned}
\boldsymbol{\omega}_2&=\boldsymbol{\omega}_1+\boldsymbol{u}_2\dot{\theta}_2,\\
\boldsymbol{\omega}_3&=\boldsymbol{\omega}_2+\boldsymbol{\omega}_3^{(r)},\\
\boldsymbol{\omega}_4&=\boldsymbol{\omega}_3+\boldsymbol{u}_4\dot{\theta}_4,\\
\boldsymbol{\omega}_5&=\boldsymbol{\omega}_1+\boldsymbol{u}_5\dot{\theta}_5.
\end{aligned}\tag{2.9}$$

A similar process to that of the previous example yields the translational velocities as

$$\begin{aligned}
\dot{\boldsymbol{r}}_2&=\dot{\boldsymbol{r}}_1-\tilde{\boldsymbol{d}}_{21}\boldsymbol{\omega}_1-\tilde{\boldsymbol{d}}_{22}\boldsymbol{u}_2\dot{\theta}_2,\\
\dot{\boldsymbol{r}}_3&=\dot{\boldsymbol{r}}_1-\tilde{\boldsymbol{d}}_{31}\boldsymbol{\omega}_1-\tilde{\boldsymbol{d}}_{32}\boldsymbol{u}_2\dot{\theta}_2-\tilde{\boldsymbol{d}}_{33}\boldsymbol{\omega}_3^{(r)},\\
\dot{\boldsymbol{r}}_4&=\dot{\boldsymbol{r}}_1-\tilde{\boldsymbol{d}}_{41}\boldsymbol{\omega}_1-\tilde{\boldsymbol{d}}_{42}\boldsymbol{u}_2\dot{\theta}_2-\tilde{\boldsymbol{d}}_{43}\boldsymbol{\omega}_3^{(r)}-\tilde{\boldsymbol{d}}_{44}\boldsymbol{u}_4\dot{\theta}_4,\\
\dot{\boldsymbol{r}}_5&=\dot{\boldsymbol{r}}_1-\tilde{\boldsymbol{d}}_{51}\boldsymbol{\omega}_1-\tilde{\boldsymbol{d}}_{55}\boldsymbol{u}_5\dot{\theta}_2,
\end{aligned}\tag{2.10}$$

where vectors $\boldsymbol{d}_{ij}$'s are shown in Fig. 2.5. From Eqs. (2.9) and (2.10), the vector of absolute velocities of the system can be written in terms of the vector of joint velocities as

$$\begin{bmatrix} \dot{r}_1 \\ \omega_1 \\ \dot{r}_2 \\ \omega_2 \\ \dot{r}_3 \\ \omega_3 \\ \dot{r}_4 \\ \omega_4 \\ \dot{r}_5 \\ \omega_5 \end{bmatrix} = \begin{bmatrix} I & 0 & 0 & 0 & 0 & 0 \\ 0 & I & 0 & 0 & 0 & 0 \\ I & -\tilde{d}_{21} & -\tilde{d}_{22}u_2 & 0 & 0 & 0 \\ 0 & I & u_2 & 0 & 0 & 0 \\ I & -\tilde{d}_{31} & -\tilde{d}_{32}u_2 & -\tilde{d}_{33} & 0 & 0 \\ 0 & I & u_2 & I & 0 & 0 \\ I & -\tilde{d}_{41} & -\tilde{d}_{42}u_2 & -\tilde{d}_{43} & -\tilde{d}_{44}u_4 & 0 \\ 0 & I & u_2 & I & u_4 & 0 \\ I & -\tilde{d}_{51} & 0 & 0 & 0 & -\tilde{d}_{55}u_5 \\ 0 & I & 0 & 0 & 0 & u_5 \end{bmatrix} \begin{bmatrix} \dot{r}_1 \\ \omega_1 \\ \dot{\theta}_2 \\ \omega_3^{(r)} \\ \dot{\theta}_4 \\ \dot{\theta}_5 \end{bmatrix}$$

From the above equation we have

$$B = \begin{bmatrix} I & 0 & 0 & 0 & 0 & 0 \\ 0 & I & 0 & 0 & 0 & 0 \\ I & -\tilde{d}_{21} & -\tilde{d}_{22}u_2 & 0 & 0 & 0 \\ 0 & I & u_2 & 0 & 0 & 0 \\ I & -\tilde{d}_{31} & -\tilde{d}_{32}u_2 & -\tilde{d}_{33} & 0 & 0 \\ 0 & I & u_2 & I & 0 & 0 \\ I & -\tilde{d}_{41} & -\tilde{d}_{42}u_2 & -\tilde{d}_{43} & -\tilde{d}_{44}u_4 & 0 \\ 0 & I & u_2 & I & u_4 & 0 \\ I & -\tilde{d}_{51} & 0 & 0 & 0 & -\tilde{d}_{55}u_5 \\ 0 & I & 0 & 0 & 0 & u_5 \end{bmatrix} \quad (30\times 12) \tag{2.11}$$

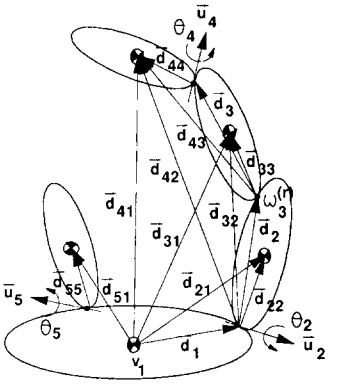

Fig. 2.5 A schematic presentation of a double-wishbone suspension system for the joint coordinates

The structare of matrix $\boldsymbol{B}$ in Eq. (2.8) or (2.11) shows that $\boldsymbol{B}$ can be constructed from small block matrices $\boldsymbol{B}_{ij}$. Table 2.1 shows $\boldsymbol{B}_{ij}$ matrices for a variety of kinematic joints. For automatic construction of $\boldsymbol{B}$, the negative integer entries ($g_{ij} < 0$) in the secondary path matrix $\boldsymbol{I}_e^*$ are replaced by their corresponding $\boldsymbol{B}_{ij}$ block matrices

Table 2.2 Block matrix $\dot{\boldsymbol{B}}_{ij}$

Type of Joint j	ID Symbols	Matrix Size	$\dot{\boldsymbol{B}}_{ij}$
Floating Base Body	$\dot{\boldsymbol{F}}_{ij}$	6×6	$\begin{bmatrix} 0 & -\dot{\tilde{d}}_{ij} \\ 0 & 0 \end{bmatrix}$
Spherical Joint	$\dot{\boldsymbol{S}}_{ij}$	6×3	$\begin{bmatrix} -\dot{\tilde{d}}_{ij} \\ 0 \end{bmatrix}$
Revolute Joint	$\dot{\boldsymbol{R}}_{ij}$	6×1	$\begin{bmatrix} -\dot{\tilde{d}}_{ij}u_j - \tilde{d}_{ij}\tilde{\omega}_j u_j \\ \tilde{\omega}_j u_j \end{bmatrix}$
Prismatic Joint	$\dot{\boldsymbol{P}}_{ij}$	6×1	$\begin{bmatrix} \tilde{\omega} u_j \\ 0 \end{bmatrix}$
Rev.-Rev. Joint	$\dot{\boldsymbol{C}}_{ij}^{R-R}$	6×2	$\begin{bmatrix} -\dot{\tilde{d}}_{ij}^{(1)}u_j^{(1)} - \tilde{d}_{ij}^{(1)}\tilde{\omega}_j u_j^{(1)} & -\dot{\tilde{d}}_{ij}^{(2)}u_j^{(2)} - \tilde{d}_{ij}^{(2)}\tilde{\omega}_j u_j^{(2)} \\ \tilde{w}_j u_j^{(1)} & \tilde{\omega}_j u_j^{(2)} \end{bmatrix}$
Pri.-Rev. Joint	$\dot{\boldsymbol{C}}_{ij}^{P-R}$	6×2	$\begin{bmatrix} \tilde{\omega}_j u_j^{(1)} & -\dot{\tilde{d}}_{ij}^{(2)}u_j^{(2)} - \tilde{d}_{ij}^{(2)}\tilde{\omega}_j u_j^{(2)} \\ 0 & \omega_j u_j^{(2)} \end{bmatrix}$
Rev.-Pri. Joint	$\dot{\boldsymbol{C}}_{ij}^{R-P}$	6×2	$\begin{bmatrix} -\dot{\tilde{d}}_{ij}^{(1)}u_j^{(1)} - \tilde{d}_{ij}^{(1)}\tilde{\omega}_j u_j^{(1)} & \tilde{\omega}_j u_j^{(2)} \\ \tilde{\omega}_j u_j^{(1)} & 0 \end{bmatrix}$

from Table 2.1. Then, the zero entries ($g_{ij}=0$) in the secondary path matrix I_s^* are replaced by their corresponding zero matrices. For the first and second examples, Eqs. (2.4) and (2.5) give rise to Eqs. (2.8) and (2.11) respectively.

Since matrix B can be described and constructed systematically, matrix $\dot{B}$ can also be constructed systematically. Table 2.2 shows $\dot{B}_{ij}$ block matrices for several kinematic joints. Note that $\dot{d}_{ij}$ can be described as $\dot{d}_{ij}=\dot{r}_i-\dot{r}_j+\tilde{\omega}_j d_{jj}$.

4. Generalized Inertia Matrix

In Part 1 of this paper, it is shown that the generalized inertia matrix $\bar{M}$ can be expressed as

$$\bar{M}=B^T M B \tag{2.12}$$

where M is a quasi-diagonal matrix, $M=\text{diag}[M_1, M_2, \cdots, M_b]$ and $M_i \equiv \text{diag}[m_i I, J_i]$; $i=1, \cdots, b$. Here, m_i is the mass of body i and J_i is the inertia tensor described in the xyz reference frame. The generalized inertia matrix $\bar{M}$ is a symmetric matrix and can be determined numerically using Eq. (2.12). However, the elements of $\bar{M}$ can also be determined directly if we consider the product of $B^T M B$ in explicit form.

Assume that matrix B is constructed from block matrices as

$$B=\begin{bmatrix} B_{11} & & & & & \\ B_{21} & B_{22} & & & & \\ B_{31} & B_{32} & B_{33} & & & \\ \cdot & \cdot & \cdot & \cdot & & \\ \cdot & \cdot & \cdot & & \cdot & \\ \cdot & \cdot & \cdot & & & \cdot \end{bmatrix}$$

Then, the product $B^T M B$ can be expressed as

$$\bar{M}=\begin{bmatrix} \sum_{i=1}^{b} B_{i1}^T M_i B_{i1} & \sum_{i=2}^{b} B_{i1}^T M_i B_{i2} & \sum_{i=3}^{b} B_{i1}^T M_i B_{i3} \cdots \\ \sum_{i=2}^{b} B_{i2}^T M_i B_{i1} & \sum_{i=2}^{b} B_{i2}^T M_i B_{i2} & \sum_{i=3}^{b} B_{i2}^T M_i B_{i3} \\ \sum_{i=3}^{b} B_{i3}^T M_i B_{i1} & \sum_{i=3}^{b} B_{i3}^T M_i B_{i2} & \sum_{i=3}^{b} B_{i3}^T M_i B_{i3} \\ \cdot & \cdot & \cdot \quad \cdot \\ \cdot & \cdot & \cdot \quad \cdot \\ \cdot & \cdot & \cdot \quad \cdot \end{bmatrix}$$

This matrix has a structure resembling a quarter-pyramid as shown in Fig. 2.6. The pyramid is composed of submatrices $\bar{M}_i$; $i=1, \cdots, b$, where

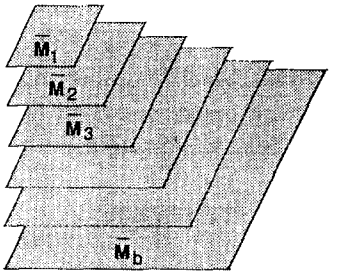

Fig. 2.6 A quarter pyramid structure of the generalized inertia matrix

$$\bar{M}_1=\begin{bmatrix} B_{11}^T M_1 B_{11} \end{bmatrix},$$

$$\bar{M}_2=\begin{bmatrix} B_{21}^T M_2 B_{21} & B_{21}^T M_2 B_{22} \\ B_{22}^T M_2 B_{21} & B_{22}^T M_2 B_{22} \end{bmatrix},$$

$$\bar{m}_3=\begin{bmatrix} B_{31}^T M_3 B_{31} & B_{31}^T M_3 B_{32} & B_{31}^T M_3 B_{33} \\ B_{32}^T M_3 B_{31} & B_{32}^T M_3 B_{32} & B_{32}^T M_3 B_{33} \\ B_{33}^T M_3 B_{31} & B_{33}^T M_3 B_{32} & B_{33}^T M_3 B_{33} \\ & \vdots & \end{bmatrix}.$$

Note that all of these submatrices are symmetric.

5. Conclusion

The joint coordinate method employs a linear velocity transformation matrix between the joint and the absolute velocities of a multibody system. This matrix is automatically constructed from block matrices and a path matrix representing the system kinematics and topology. This method generates a small or even a minimal set of equations of motion necessary for the forward or inverse dynamics analysis of multibody systems. Furthermore, the necessary equations for static equilibrium or design sensitivity analysis are also obtained as a small or a minimal set of equations.

The joint coordinate method gives rise to easy computer implementation of the algorithms, automatic generation of the equations, and efficient numerical solution. Since the joint coordinates are physical coordinates, this method provides an easy interpretation between the actual system and its mathematical or computer model. The effective

generalized masses and generalized forces can be determined explicitly in terms of block matrices and vector forms, which in turn provides a powerful basis for the design sensitivity analysis and parallel processing computation.

References

Gim, G. and Nikravesh, P.E., 1993, "Joint Coordinate Method for Analysis and Design of Multibody Systems: Part 1. System Equations," KSME Journal, Vol. 7, No. 1, pp. 14~25.

Kim, S.S. and Vanderploeg, M.J., 1986, "A General and Efficient Method for Dynamic Analysis of Mechanical Systems Using Velocity Transformations," ASME Journal of Mechanisms, Transmissions, and Automation in Design, Vol. 108, No. 2, pp. 176~182.